

Supporting Information for ” Alongshore winds force warm Atlantic Water toward Helheim Glacier in southeast Greenland”

T. Snow^{1,2,3}, W. Zhang⁴, E. Schreiber⁵, W. Abdalati^{2,3}, T. Scambos²

¹Colorado School of Mines, Department of Geophysics, Golden, CO, USA

²Cooperative Institute for Research in Environmental Sciences, University of Colorado, Boulder, CO, USA

³University of Colorado Boulder, Geography Department, Boulder, CO, USA

⁴Applied Ocean Physics and Engineering Department, Woods Hole Oceanographic Institution, Woods Hole, MA, USA

⁵UNAVCO, 6350 Nautilus Drive, Boulder, CO, 80301, USA

Contents of this file

1. Text S1 to S4
2. Figures S1 to S4

Introduction The text and figures included in this supplement provide additional information and context supporting the conclusion of the main text.

Text S1. ERA-5 wind data analysis To determine the atmospheric variability associated with the Atlantic Water (AW) intrusions, we use the ERA-5 6-hourly 2-m wind field, instantaneous eastward and northward turbulent surface stresses, and mean sea level

pressure fields on a $0.5^\circ \times 0.5^\circ$ grid. From the ERA-5 U and V wind speeds and stress, we calculate alongshore winds as the velocity/stress component traveling along the principal axis of 242° from north at the shelf break. We produce a time series of wind direction and alongshore wind stress from 2010 to 2013 for comparison to the dates of the intrusions. At each time, the wind direction, speed, and stress are averaged across the mouth region of Sermilik Trough (between 64.4° - 65.0° N, -38.0° - 35.0° E; Figure 1a), where winds have the strongest correlation with changes in regional EGCC transport and the greatest impact on trough transport (Harden et al., 2014; Le Bras et al., 2018). Piteraqaq events (or Downslope Wind Events) are identified as >10 m/s winds between 270 and 20° (clockwise) averaged over the Tasiilaq region (65.5° - 65.7° N, -37.82° E- 37.42° E) following Oltmanns, Straneo, Moore, and Mernild (2014) (Figure 1a).

Text S2. Ocean mooring records The shelf and mid-fjord mooring instruments provide ocean temperature records during the AW intrusions. For the shelf mooring, we use the temperatures recorded by one instrument each year, either a Microcat SBE37SM or XR 420 RBR sensor, deployed between 262 and 301 m near the mouth of Sermilik Fjord. The mid-fjord mooring was deployed between 250-294, 324-350, 390-400, and 550-560 m depth (representing the 250, 350, 400, and 550 m records, respectively) and recorded temperatures using similar instruments as the shelf mooring (Jackson et al., 2014). Temperatures were acquired at 7.5-15 min intervals and averaged to 6-hourly.

Text S3. EGCC width and transport As a fresher water mass running along the coastline, the size of the EGCC may moderate the AW intrusions by serving as a barrier or diluting the intrusions as they cross the continental shelf (Snow et al., 2021). We use

satellite-based calculations of the EGCC width in accordance with Snow et al. (2021) to indicate the size of the EGCC. We use the MODIS Level 3 SST V2014 products (Minnett et al., 2019). MODIS SSTs were sampled from the same shelf trough transect as Snow et al. (2021) (thirteen 14x14 km sampling boxes) and the SST anomaly relative to the Irminger Current temperature was then calculated and averaged to weekly. We approximated the EGCC width along the trough by measuring the distance from the fjord mouth (65.6°N,-38.0°E) to the center of the last sampling box along the trough transect that had a SST anomaly $<-1.5^{\circ}\text{C}$ (threshold delineating between PW at the surface within the EGCC and AW from the IC; Snow et al., 2021).

We observe enhanced temperature variability at the subsurface shelf mooring ($r^2=0.40$; Figure S3) when the EGCC is wider, which is consistent with greater transport within the EGCC. A wider EGCC seasonally coincides with greater transport and a deepening of the current (Harden et al., 2014), which stratifies deeper water layers along the inner shelf. Higher variability at the mooring sensor (290 m) indicates a deeper PW/AW interface that is normally located between 150-250 m depth (Harden et al., 2014; Jackson et al., 2014). Therefore, we use EGCC width as an indicator for EGCC transport.

Text S4. Atmosphere and ocean cross-correlation analyses To investigate the linkages between atmospheric and ocean records, we smoothed all records with a 30-hour second-order Butterworth filter and performed cross-correlation analyses between them. Across the four-year record, the shelf and fjord mooring temperatures lagged alongshore wind stress by ~ 24 hours and 30 hours, respectively (Figure S4b). At these

lags, ocean temperatures negatively correlated with alongshore wind stress ($r=-0.19$, -0.22 , and -0.24 , for the shelf at 290 m, mid-fjord at 250 m and mid-fjord at 350 m depth, respectively; $p<0.001$). SSH lagged alongshore wind stress by ~ 6 hrs (Figure S4a) and ocean temperatures at each of the mooring sites had a stronger negative correlation with SSH ($r=-0.33$, -0.32 , and -0.33 , respectively; $p<0.001$) than with alongshore winds. The shelf warming followed a drop in SSH by 6 hours, while the mid-fjord warming followed the shelf SSH drop by 24 hrs (Figure S4c). These negative correlations are consistent with a downwelling-to-upwelling switch in coastal conditions and the observed lags are consistent with (Jackson et al., 2014).

References

- Harden, B., Straneo, F., & Sutherland, D. (2014). Moored observations of synoptic and seasonal variability in the East Greenland Coastal Current. *Journal of Geophysical Research: Oceans*, *119*(12), 8838–8857. doi: 10.1002/2014JC010134
- Jackson, R. H., Straneo, F., & Sutherland, D. A. (2014). Externally forced fluctuations in ocean temperature at Greenland glaciers in non-summer months. *Nature Geoscience*, *7*(7), 503–508. doi: 10.1038/ngeo2186
- Le Bras, I., Straneo, F., Holte, J., & Holliday, P. N. (2018). Seasonality of Freshwater in the East Greenland Current System From 2014 to 2016. *Journal of Geophysical Research: Oceans*. doi: 10.1029/2018JC014511
- Minnett, P., Alvera-Azcárate, A., Chin, T., Corlett, G., Gentemann, C., Karagali, I., ... Vazquez-Cuervo, J. (2019). Half a century of satellite remote sensing of sea-surface temperature. *Remote Sensing of Environment*, *233*, 111366. doi: 10.1016/

j.rse.2019.111366

Oltmanns, M., Straneo, F., Moore, G., & Mernild, S. (2014). Strong Downslope Wind Events in Ammassalik, Southeast Greenland. *Journal of Climate*, 27(3), 977–993.

doi: 10.1175/JCLI-D-13-00067.1

Snow, T., Straneo, F., Holte, J., Grigsby, S., Abdalati, W., & Scambos, T. (2021). More than skin deep: sea surface temperature as a means of inferring Atlantic Water variability on the southeast Greenland continental shelf near Helheim Glacier. *Journal of Geophysical Research: Oceans*.

doi: <https://www.essoar.org/doi/abs/10.1002/essoar.10503490.1>

Table S1: AW intrusions identified from MODIS visible imagery and ERA-5 alongshore wind stress.

Beginning of Table S1			
Date Time	Image Date	Piteraqaq [T/F]	EGCC width [km]
2010-01-23 18:00:00	2010-01-24	1	75.5
2010-02-16 06:00:00	2010-02-17	0	75.5
2010-03-05 06:00:00	2010-03-05	1	75.5
2010-03-11 18:00:00	2010-03-12	0	90.1
2010-03-14 18:00:00	2010-03-15	0	90.1
2010-03-25 18:00:00	2010-03-26	0	60.6
2010-03-30 06:00:00	2010-03-31	0	60.6
2010-04-06 12:00:00	2010-04-06	0	90.1
2010-04-11 12:00:00	2010-04-11	0	90.1
2010-04-16 18:00:00	2010-04-16	0	90.1
2010-04-30 12:00:00	2010-04-30	0	75.5
2010-05-05 18:00:00	2010-05-06	0	75.5
2011-01-24 18:00:00	2011-01-24	0	75.5
2011-02-15 12:00:00	2011-02-17	0	46.0
2011-02-25 18:00:00	2011-02-26	1	60.6
2011-03-03 00:00:00	2011-03-03	0	90.1
2011-03-06 06:00:00	2011-03-06	1	90.1
2011-03-25 18:00:00	2011-03-26	0	110.3
2011-04-11 00:00:00	2011-04-11	0	110.3
2011-04-14 06:00:00	2011-04-14	0	110.3
2011-04-19 06:00:00	2011-04-19	1	110.3
2011-05-08 18:00:00	2011-05-09	0	75.5
2011-05-23 12:00:00	2011-05-23	0	75.5
2011-06-01 18:00:00	2011-06-01	0	90.1
2012-01-25 18:00:00	2012-01-26	0	75.5
2012-01-29 12:00:00	2012-01-29	0	75.5
2012-02-09 18:00:00	2012-02-10	0	31.4
2012-02-15 00:00:00	2012-02-16	0	90.1
2012-03-09 06:00:00	2012-03-09	0	130.5
2012-03-14 00:00:00	2012-03-14	0	110.3
2012-03-27 06:00:00	2012-03-27	0	110.3
2012-04-03 00:00:00	2012-04-03	0	90.1
2012-04-05 18:00:00	2012-04-06	0	90.1
2012-04-13 00:00:00	2012-04-13	0	150.7
2012-04-20 06:00:00	2012-04-20	0	60.6
2012-04-27 06:00:00	2012-04-28	0	60.6
2012-04-30 12:00:00	2012-05-01	0	60.6
2012-05-02 18:00:00	2012-05-03	0	60.6

Continuation of Table S1			
Date Time	Image Date	Piteraqaq [T/F]	EGCC width [km]
2012-05-25 12:00:00	2012-05-26	0	110.3
2012-06-11 06:00:00	2012-06-11	0	-
2012-06-15 00:00:00	2012-06-16	0	-
2012-06-18 00:00:00	2012-06-19	0	110.3
2012-06-25 00:00:00	2012-06-25	0	-
2013-01-28 18:00:00	2013-01-28	0	46.0
2013-02-04 12:00:00	2013-02-04	0	75.5
2013-03-01 06:00:00	2013-03-01	1	90.1
2013-03-12 00:00:00	2013-03-12	0	60.6
2013-03-21 18:00:00	2013-03-22	0	90.1
2013-04-08 18:00:00	2013-04-08	0	75.5
2013-04-23 00:00:00	2013-04-24	0	75.5
2013-05-08 00:00:00	2013-05-08	0	90.1
2013-05-20 12:00:00	2013-05-20	0	60.6
2013-06-16 00:00:00	2013-06-16	0	110.3

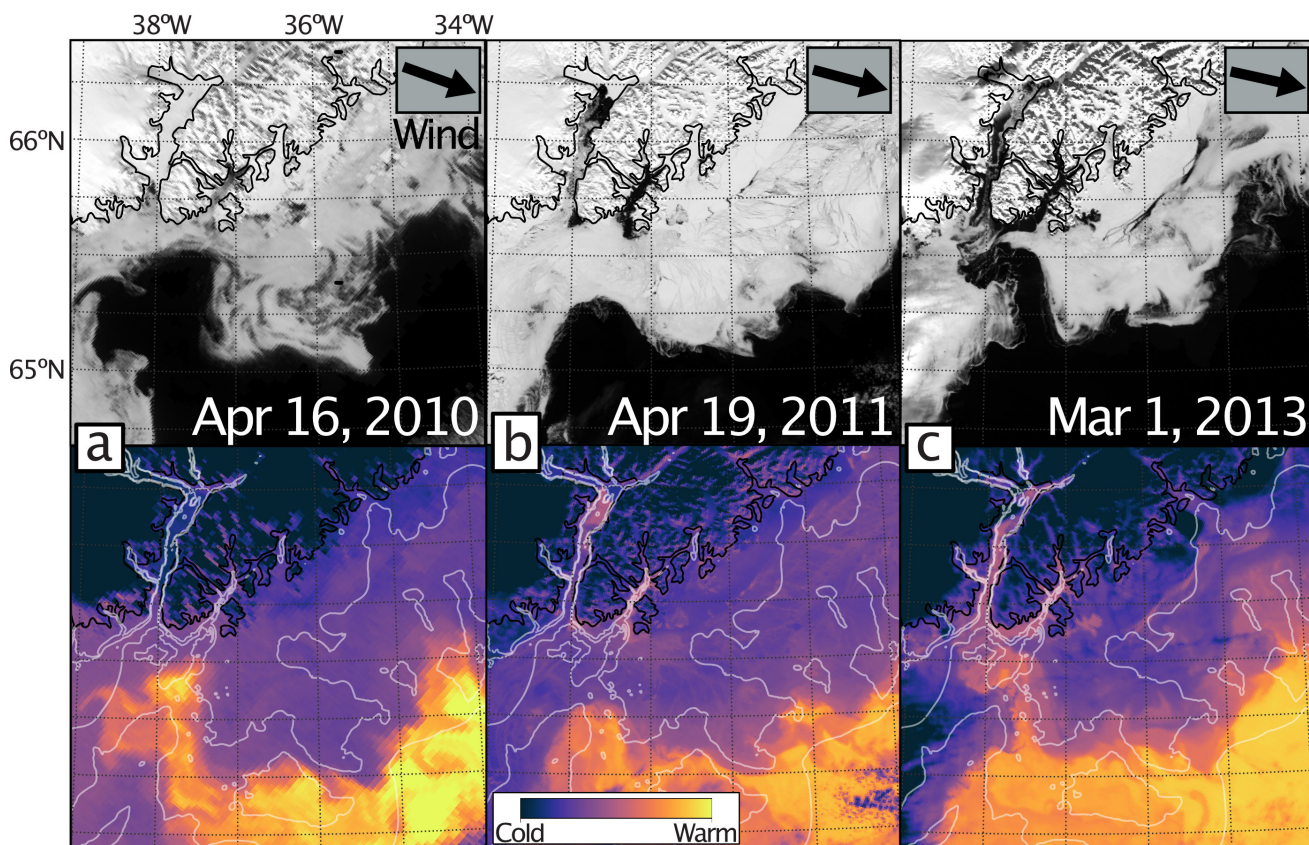


Figure S1. Three intrusions observed in MODIS imagery in the visible spectrum (top) and Band 31 (thermal infrared)-derived brightness temperatures (bottom) shown for (a) April 16, 2010, (b) April 19, 2011, and (c) March 1, 2013. Black arrows indicate wind direction.

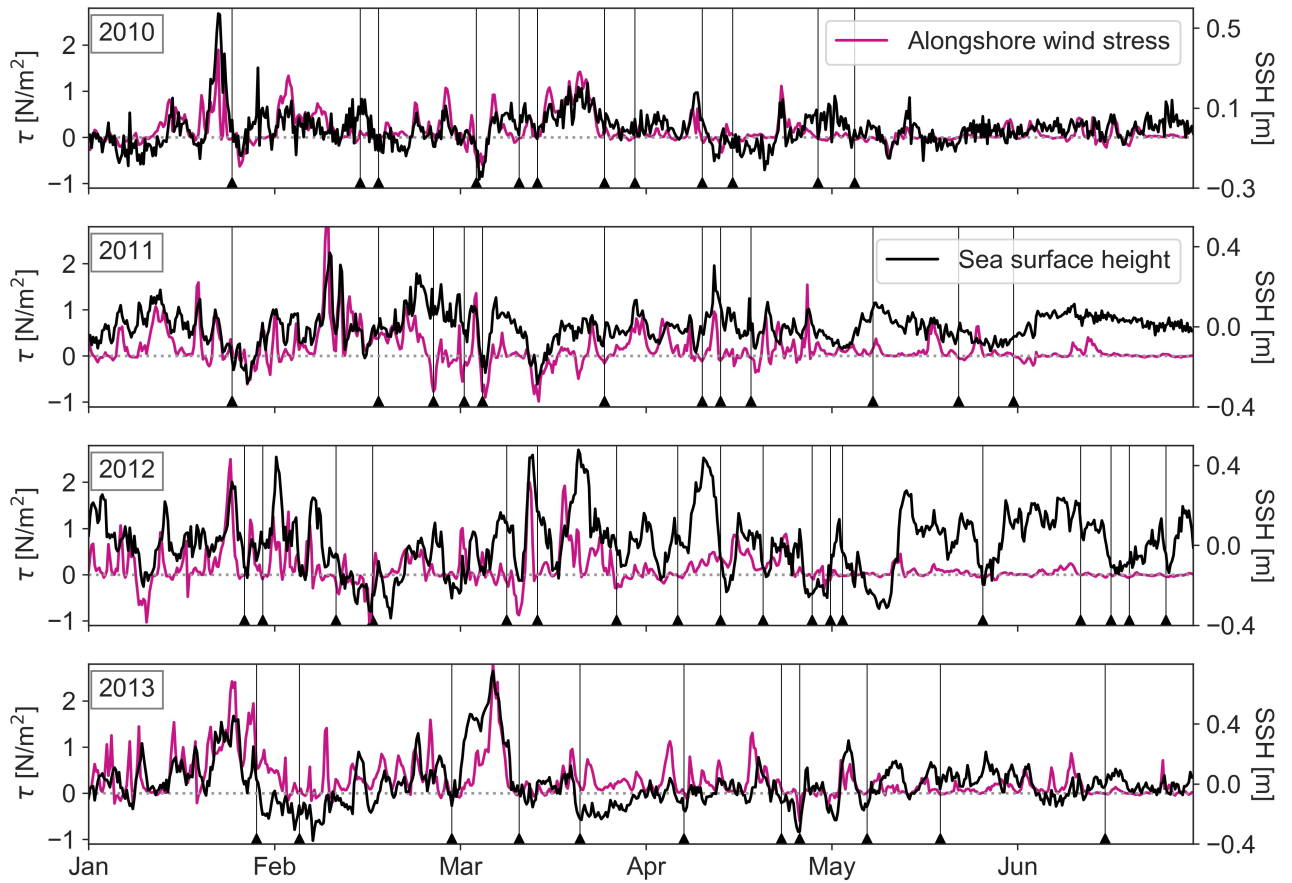


Figure S2. The dates of all MODIS-observed intrusions used in this study (vertical lines) in comparison to alongshore wind stress (purple lines; positive means northeasterly) and continental shelf sea surface height (SSH; black lines) records. The records span from January through June for each year.

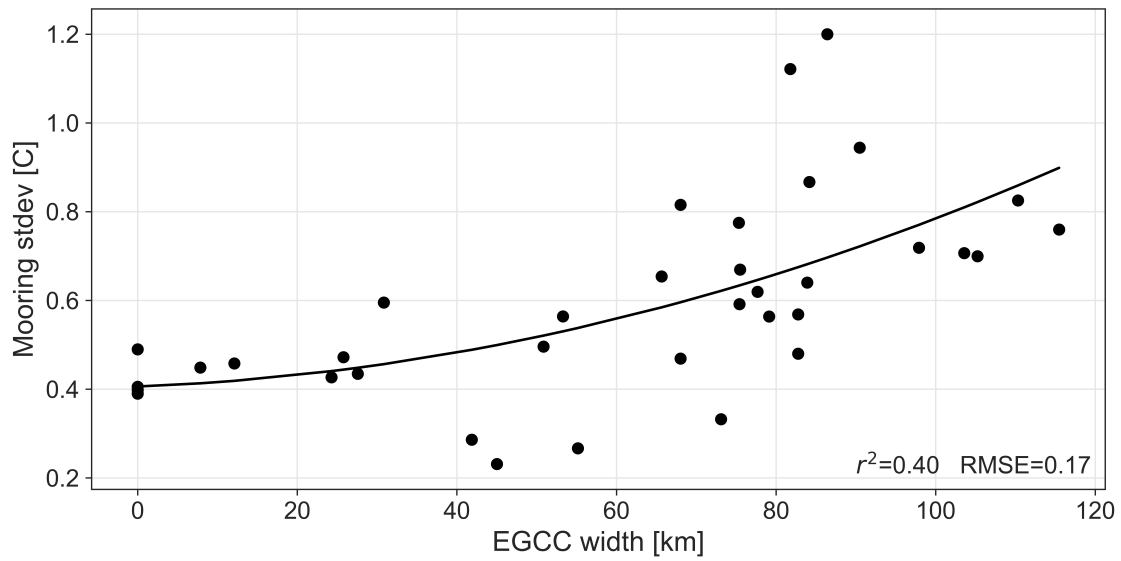


Figure S3. Standard deviation of monthly-aggregated moored subsurface ocean temperatures in comparison to sea surface temperature-derived EGCC width (circles). The second-order polynomial for the data (line), r^2 , and root mean square error (RMSE) are shown.

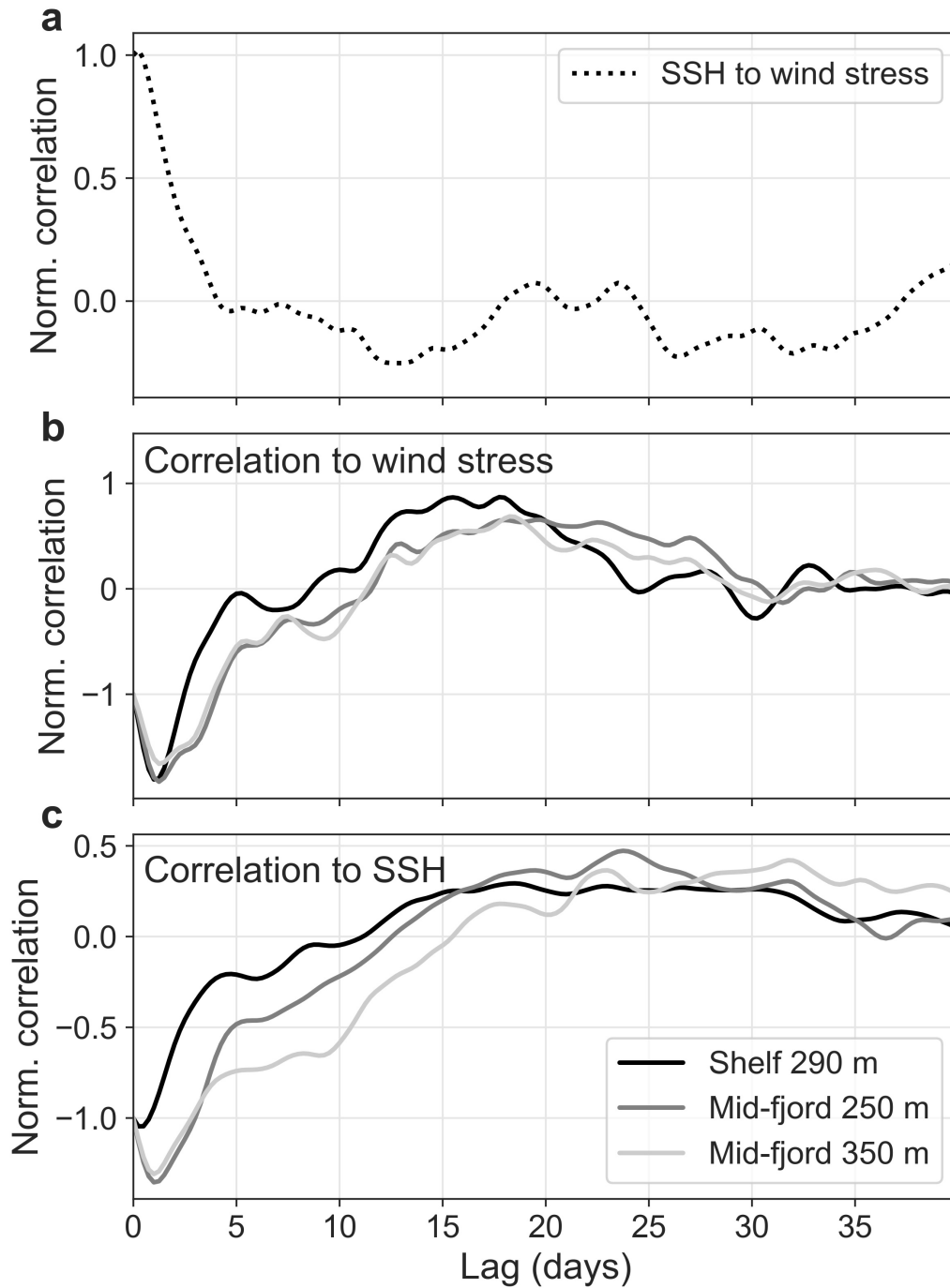


Figure S4. Cross-correlations between alongshore wind stress, sea surface height (SSH), and mooring temperature records. (a) Cross correlation of SSH and alongshore winds. Cross correlation of the shelf 290 m (black), mid-fjord 250 m (dark gray), and mid-fjord 350 m (light gray) mooring temperature records with (b) the alongshore wind stress and (c) SSH. All records were smoothed with a 30-hour second-order Butterworth filter.